On-Line Concentration of Neutral Analytes for Micellar Electrokinetic Chromatography. 3. Stacking with Reverse Migrating Micelles

ARTICLE *in* ANALYTICAL CHEMISTRY · JANUARY 1998

Impact Factor: 5.64 · DOI: 10.1021/ac9706281 · Source: PubMed

2 AUTHORS, INCLUDING:

Joselito P Quirino
University of Tasmania
102 PUBLICATIONS **4,896** CITATIONS

SEE PROFILE

Anal. Chem. **1998,** *70,* 149−157

On-Line Concentration of Neutral Analytes for Micellar Electrokinetic Chromatography. 3. Stacking with Reverse Migrating Micelles

Joselito P. Quirino* and Shigeru Terabe

Faculty of Science, Himeji Institute of Technology, Kamigori, Hyogo, Japan 678-12

On-line concentration of neutral analytes by sample stacking in reversed migration micellar electrokinetic chromatography is presented. Micellar separation solutions of sodium dodecyl sulfate are prepared with acidic buffers to reverse the direction of the migration velocity of neutral analytes owing to a reduced electroosmotic flow. Samples are prepared in nonmicellar matrixes of low conductivity (i.e., water, diluted buffer, or dilute organic/aqueous solvent) to achieve field enhancement in the sample zone. Without polarity switching inherent in large-volume sample stacking, narrowing of analyte bands, removal of sample matrix, and separation of focused analyte bands are achieved. A model is proposed to describe the stacking technique and is supported by experimental results. In addition, equations are derived to describe band broadening associated with the technique. Detector response improvements reaching a 100-fold are confirmed experimentally. Concentration detection limits on the order of low-ppb levels (S/N = 3) are realized with model steroidal compounds.

Introduced by Terabe et al. in 1984,[1] micellar electrokinetic chromatography (MEKC) is a powerful separation approach that augments the usage of electrokinetic phenomena for the separation of nonionic compounds. MEKC separations are based on the partitioning of neutral solutes between the electrokinetically moved micellar phase and the electroosmotically pumped bulk aqueous phase. One restraint of the technique is the low concentration sensitivity as a consequence of the limited optical path length for on-line UV detection and the limited volume of sample solution that can be injected. This hinders the application of MEKC in the analysis of more real samples.

Peak sharpening in capillary zone electrophoresis can be observed when ionic samples are prepared in a high-resistivity matrix.[2−8] This is commonly known as sample stacking,[2] which results from the movement of sample ions across a distinct concentration boundary found between the high-resistivity sample zone and low-resistivity separation zone. Because of field enhancement in the high-resistivity zone, the electrophoretic velocity of ions found in such a zone is much greater than that found in the low-resistivity separation zone. Therefore, sample ions narrow down into thin concentrated zones in the aforesaid boundary.

Sample stacking relies on the accelerated electrophoretic velocity of ionic sample constituents, which deters its simple transfer to MEKC for neutral sample constituents. The enhanced field does not influence neutral analytes, and thus stacking will depend on the solubilization of such analytes into the accelerated micelles. Only a few papers appeared regarding sample stacking of neutral analytes in MEKC. Liu et al. reported the use of sodium dodecyl sulfate (SDS) with concentrations slightly above the critical micelle concentration (cmc) in the sample zone by normal stacking mode (NSM) and reversed electrode polarity stacking mode (REPSM).[9] Nielson and Foley reported the use of cationic mixed micelles in the sample matrix with electrokinetic injection.[10] Recently, we improved NSM and REPSM using nonmicellar solutions of low conductivity to prepare the samples.[11,12] All these aforementioned efforts featured sample stacking of neutral analytes in the presence of high electroosmotic flow and untreated fused-silica capillaries. In our previous works, separation solutions contained high molecular mass surfactants (HMMS) or low molecular mass surfactants (LMMS) in neutral buffers. More than 1 order of magnitude improvement in concentration detection limit was realized with REPSM and almost 1 order of magnitude with NSM using HMMS.

In this particular study, we show another simple yet effective procedure for stacking neutral analytes in the presence of low electroosmotic flow. The electroosmotic flow is reduced using low-pH separation solutions. Although MEKC at low pH in bare silica capillaries was considered inferior due to poor reproducibility,[13] the advent of fine commercial instruments capable of running automated cleaning schemes solved this limitation. Phenols, naphthalenes, and steroids are used as test compounds. A model is developed to describe the stacking and separation processes and is supported by some experimental results. More-

(1) Terabe, S.; Otsuka, K.; Ichihara, K.; Tsuchiya, A.; Ando, T. *Anal. Chem.* **1984**, *56*, 111−3.
(2) Chien, R. L.; Burgi, D. S. *Anal. Chem.* **1992**, *64*, 489A−96A.
(3) Burgi, D. S.; Chien, R. L. *J. Microcolumn Sep.* **1991**, *3*, 199−202.
(4) Burgi, D. S.; Chien, R. L. *Anal. Chem.* **1991**, *63*, 2042−7.
(5) Chien, R. L.; Burgi, D. S. *J. Chromatogr., A* **1991**, *559*, 141−52.
(6) Chien, R. L.; Burgi, D. S. *J. Chromatogr., A* **1991**, *559*, 153−61.
(7) Chien, R. L.; Burgi, D. S. *Anal. Chem.* **1992**, *64*, 1046−50.
(8) Burgi, D. S. *Anal. Chem.* **1993**, *65*, 3726−9.
(9) Liu, Z; Sam, P; Sirimanne, P. C.; McClure, J.; Grainger, J.; Patterson, D. G. *J. Chromatogr., A* **1994**, *673*, 125−32.
(10) Nielson, K. R.; Foley, J. P. *J. Chromatogr., A* **1994**, *686*, 283−91.
(11) Quirino, J. P.; Terabe, S. *J. Chromatogr., A* **1997**, *781*, 119−28.
(12) Quirino, J. P.; Terabe, S. *J. Chromatogr., A*, in press.
(13) Otsuka, K.; Terabe, S. *J. Microcolumn Sep.* **1989**, *1*, 150−4.

S0003-2700(97)00628-8 CCC: $14.00
Published on Web 01/01/1998

over, equations are derived to explain band broadening observed with the method.

EXPERIMENTAL SECTION

Apparatus. All capillary electropherograms were obtained from a Hewlett Packard 3D capillary electrophoresis system (Waldbronn, Germany). All experiments were performed in fused-silica capillaries of 50 μm i.d. and 375 μm o.d. obtained from Polymicro Technologies (Phoenix, AZ). Capillaries were thermostated at 20 °C. Optimum detection wavelengths for each analyte were selected using spectral absorbance data recorded using a diode array detector. Conductivities were measured using a Horiba ES-12 conductivity meter (Kyoto, Japan).

Reagents and Solutions. All reagents were purchased in the highest grade possible from Nacalai Tesque (Kyoto, Japan). Water was purified with a Milli-Q system (Millipore, Bedford, MA). Stock solutions of 0.5 M SDS were prepared every week with purified water. Low-pH micellar background solutions (BGS) were prepared by dilution of the SDS stock solution with appropriate phosphate buffers. Urea or γ-cyclodextrin was added to improve the separation of test phenols and steroids. Fresh BGSs were prepared every day to prevent migration time reproducibility problems (due to changes in SDS concentration, change in solution bulk viscosity, etc.) that may occur when old solutions are used. SDS can hydrolyze to form dodecanol in acidic media.[14]

Stock solutions of phenol and naphthalene derivatives were prepared with purified water. In some cases, a few milliliters of ethanol was added to aid in the dissolution of some hydrophobic phenol derivatives. Stock solutions of the steroids studied were prepared with 95% ethanol. All sample stock solutions were diluted with purified water to procure sample solutions with analytes possessing comparable peak heights. Further dilutions with purified water were done for the construction of calibration curves in the determination of concentration detection limits. All solutions were filtered through 0.45 μm filters (Toyo Roshi, Tokyo, Japan) prior to capillary electrophoresis experiments.

Procedure. The capillary was rinsed prior to use with 1 M NaOH (10 min), followed by methanol (5 min), purified water (5 min), and finally BGS (5 min). Test analytes prepared basically in water were injected into the capillary at the cathodic end using pressure (50 mbar or 1 bar). The applied injection times were much longer than usual hydrodynamic injection (typically 1 or 2 s). Voltage was applied at negative polarity with the BGS in the cathodic and anodic vials. The capillary was flushed, between consecutive analyses to ensure repeatability, with 1 M NaOH (1 min), followed by methanol (1 min), 0.1 M NaOH (1 min), purified water (2 min), and finally BGS (2 min). Other conditions are specified in the text or figures.

RESULTS AND DISCUSSION

Stacking with the Reverse Migrating Micelles-Micellar Electrokinetic Chromatography (SRMM-MEKC) Model. Sample solutions prepared in low-conductivity matrixes (S) are injected as long plugs into the capillary previously filled with the BGS (see Figure 1A). Sample solutions are injected at the cathodic end, and voltages are applied at negative polarity such that the electrophoretic velocity of the micelles is directed toward the detector. Note that the electrophoretic velocity of micelles at low pH is greater than the electroosmotic flow velocity[13] due to protonation of silanol groups at the inner surface of the capillary that reduces the zeta potential. The inlet (cathodic) and outlet (anodic) vials contain the BGS. The S region is the unshaded area with neutral analytes a (a_x, a_y, a_z). The BGS region is the heavily shaded area.

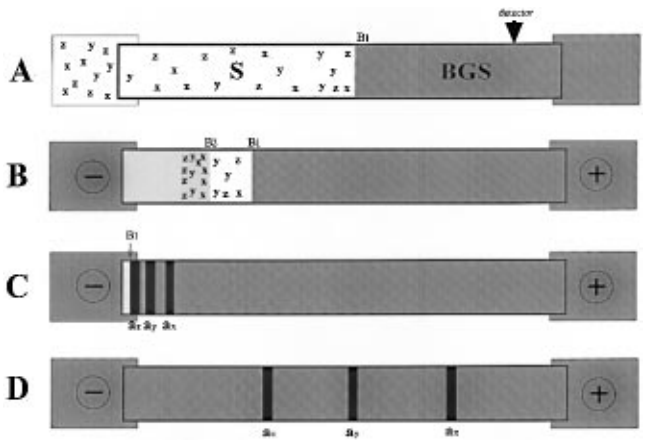

Figure 1. Evolution of micelles and neutral analytes in the sample solution (S) zone and separation solution (BGS) zone during and after stacking at acidic pH: A, starting situation; B, high-velocity micelles in the S zone emanating from the cathodic vial carry the neutral analytes to the concentration boundary (B_1) in the order of decreasing retention factor $k(a_x) > k(a_y) > k(a_z)$; C, neutral analytes after stacking leave B_1 prior to the removal of the sample matrix due to electrophoresis in the BGS zone; D, neutral analyte zones migrate toward the detector and continue to separate. Shaded parts indicate the presence of micelles.

After a certain time as shown in Figure 1B, micelles from the cathodic vial enter the capillary (lightly shaded part of the S region) and carry with them neutral analytes found in the S region toward the anodic end. High retention factor compounds travel faster than low retention factor compounds. Buffer anions also enter the S region. Furthermore, in Figure 1B, the sample matrix is being pumped out of the capillary to the cathodic vial by the electroosmotic flow and is being replaced by the BGS coming from the anodic vial. After the stacking of neutral analytes in the concentration boundary (B_1) and prior to the complete removal of the sample matrix, focused analyte bands separate from B_1 (see Figure 1C). Finally in Figure 1D, the sample matrix is completely removed from the column. Subsequently, separation and detection of stacked zones occur. No polarity switching is involved.

Experimental Verification of the SRMM-MEKC Model. (a) Initial Behavior of Micelles. With the configuration in Figure 1A, the migration velocity of micelles in both the S region, ν_{mc}(S), and the BGS region, ν_{mc}(BGS), is the sum of two vector quantities, i.e., the averaged bulk velocity of the electroosmotic flow, ν_{eof}(av), and the electrophoretic velocity of the micelle in the S region, ν_{ep}(mc,S), and BGS region, ν_{ep}(mc,BGS), respectively (eqs 1 and 2).[11] The electrophoretic velocities of the micelles in

$$\nu_{mc}(S) = \nu_{eof}(av) + \nu_{ep}(mc,S) \quad (1)$$

$$\nu_{mc}(BGS) = \nu_{eof}(av) + \nu_{ep}(mc,BGS) \quad (2)$$

the two regions are given by eqs 3 and 4. Following ref 2, the

(14) Kurz, J. L. *J. Phys. Chem.* **1962**, *66*, 2239.

$$\nu_{ep}(\mathrm{mc,S}) = \mu_{ep}(\mathrm{mc})E_S \quad (3)$$

$$\nu_{ep}(\mathrm{mc,S}) = \mu_{ep}(\mathrm{mc})E_{BGS} \quad (4)$$

field strengths in the S region (E_S) and BGS region (E_{BGS}) are given by eqs 5 and 6, respectively. E_0 is equal to V/L (constant

$$E_S = \gamma E_0/[\gamma x + (1 - x)] \quad (5)$$

$$E_{BGS} = E_0/[\gamma x + (1 - x)] \quad (6)$$

voltage V applied across a capillary with length L), γ is the enhancement factor equal to the resistivity ratio of S and BGS, and x is the fraction of the capillary filled with S. Both the field strengths in the S and BGS regions increase with the decrease in x based on eqs 5 and 6, but to a greater extent in the S region with a factor γ. A corresponding increase in ν_{ep}(mc,S) and ν_{ep}(mc,BGS) will be the result.

The bulk electroosmotic velocity is given by[2]

$$\nu_{eof}(\mathrm{av}) = \frac{\gamma x \nu_{eof}(\mathrm{S}) + (1 - x)\nu_{eof}(\mathrm{BGS})}{\gamma x + (1 - x)} \quad (7)$$

where ν_{eof}(S) and ν_{eof}(BGS) are the electroosmotic flow velocities of S and BGS, respectively, measured in their homogenous systems. With the decrease in x during the stacking process, ν_{eof}(av) changes from ν_{eof}(S) to ν_{eof}(BGS). Basically, ν_{ep}(mc,S), ν_{ep}(mc,BGS), and ν_{eof}(av) change with the reduction of x, but the change in ν_{eof}(av) and ν_{ep}(mc,BGS) is not large compared to the change in ν_{ep}(mc,S).

We now mention x_{max}, which is the maximum fraction of the capillary filled with S that will permit the movement of micelles from the cathodic vial into the capillary.[12] For values of x lower than x_{max}, ν_{mc}(S) is negative or toward the anode since ν_{ep}(mc,S) is greater in magnitude than ν_{eof}(av). Micelles from the cathodic vial therefore enter the capillary as shown in Figure 1B. The stacking of neutral analytes proves the migration of micelles into the S region, as will be shown later. Because of low field strength in the BGS zone at this stage, ν_{mc}(BGS) is positive or toward the cathode since ν_{eof}(av) is much greater in magnitude than ν_{ep}(mc,BGS). Micelles in the injected BGS region therefore migrate toward the cathode (heavily shaded area in Figure 1A moves to the left as shown in Figure 1B). The migration direction of micelles at this stage in the BGS zone is illustrated in Figure 2. A solution of phenanthrene in the BGS was injected at the anodic end, 8.5 cm from the detector, after a long plug of water was injected at the cathodic end, 26 cm from the detector. Water here is used to mimic S. Phenanthrene (first peak) as a marker is detected in less than 1 min. The second peak in Figure 2 will be touched upon later.

(b) The Gap Separating the Concentration Boundary and Micellar Boundary (Nonmicellar Gap). The B_1 in Figure 1A (after injection of S and prior to the application of voltage) separates into several boundaries (concentration and electrolyte boundaries) in Figure 1B. The important ones are the concentration or stacking boundary and the micellar boundary. The position of B_1 in Figure 1A is where all the boundaries are located. From here to avoid confusion, we refer to B_1 as the concentration

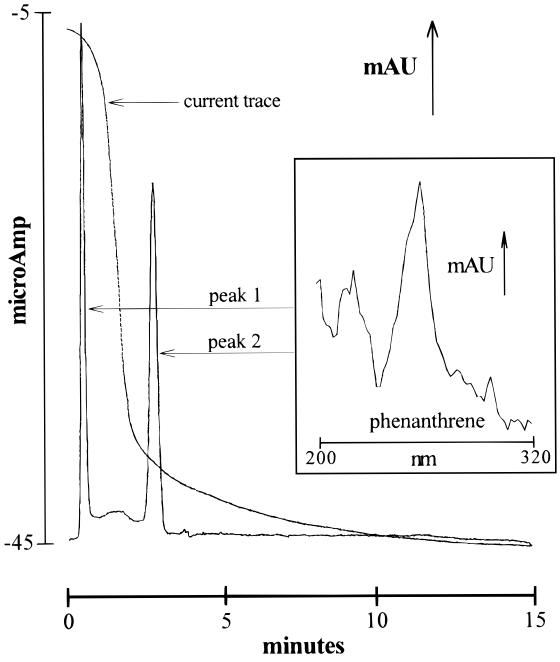

Figure 2. Effect of the low-conductivity zone on the migration velocity of micelles in the BGS during stacking: BGS, 50 mM SDS in 50 mM phosphate buffer (pH 2.5); injection, 180 s water at the cathodic end followed by 2 s injection of phenanthrene solution (prepared in the BGS) at the anodic end; voltage, −15 kV; detection, 251 nm; capillary, 43 cm (34.5 cm to the detector). The inset is an on-line recorded spectrum which is characteristic at each peak maximum.

boundary. The migration velocity of B_1 is approximately equal to ν_{eof}(av) while that of the micellar boundary is equal to ν_{mc}(BGS); thus the difference in migration velocities is equal to ν_{ep}(mc,BGS). The distance of these boundaries from each other (nonmicellar gap) in Figure 1B is then small (not depicted in this figure) and did not produce a discernable undesirable effect to the stacking procedure. The nonmicellar gap was studied by injecting a small plug of buffer before injecting S. No visible effect was observed.

When the anodic vial was filled with buffer, the current increased in magnitude due to the difference in conductivity values between the buffer and the BGS. When the capillary was filled with buffer and not the BGS, unacceptable electropherograms were obtained since the detector was calibrated with the buffer. The analytes were stacked and separated since stacking and separations are dependent on the micelles coming from the cathodic vial. Both conditions are not practical.

(c) Behavior of Neutral Analytes in the Stacking or Concentration Boundary. When B_2 reaches B_1 in Figure 1B, micelles and neutral analytes solubilized in it stack in B_1 since the experienced field drops abruptly. The electrophoretic velocity of micelles shifts from ν_{ep}(mc,S) to ν_{ep}(mc,BGS). The migration velocity difference between the stacked micelle and B_1 is also equal to ν_{ep}(mc,BGS). This small difference in migration velocities will cause the stacked micelles to leave B_1 prior to the total removal of the sample matrix. The same follows for neutral analytes solubilized in the stacked micelles (see Figure 1C). The migration velocities of a in the S region ,ν_a(S), and BGS region, ν_a(BGS), are given by eqs 8 and 9, respectively.[12]

$$\nu_a(S) = \nu_{eof}(av) + \nu_{ep}^*(a,S) \quad (8)$$

$$\nu_a(BGS) = \nu_{eof}(av) + \nu_{ep}^*(a,BGS) \quad (9)$$

where the effective electrophoretic velocities of *a* in the S region, $\nu_{ep}^*(a,S)$, and in the BGS region, $\nu_{ep}^*(a,BGS)$, are given by eqs 10 and 11, respectively.

$$\nu_{ep}^*(a,S) = \nu_{ep}(mc,S)\frac{k_S}{k_S+1} = \mu_{ep}(mc) \times \frac{\gamma E_0}{\gamma x + (1-x)}\frac{k_S}{k_S+1} \quad (10)$$

$$\nu_{ep}^*(a,BGS) = \nu_{ep}(mc,S)\frac{k_{BGS}}{k_{BGS}} = \mu_{ep}(mc) \times \frac{E_0}{\gamma x + (1-x)}\frac{k_{BGS}}{k_{BGS}+1} \quad (11)$$

Here, k_S is the retention factor in the S zone and k_{BGS} is the retention factor in the BGS zone.

The $\nu_{ep}^*(a,BGS)$ is then the migration velocity difference between the stacked *a* and B_1 that will cause the stacked *a* to separate from B_1. Figure 3A shows that separation of stacked *a* occurs prior to the complete removal of the sample matrix (ethylphenol was detected even if the current had not stabilized completely). Stability of the current is an indication that the sample matrix is completely removed from the capillary. To substantiate this observation, an additional experiment was performed wherein pressure was applied at the inlet side (toward the detector) before the sample matrix was removed from the capillary and before the analytes reached the detector (see Figure 3B). As expected, ethylphenol and phenol are detected as separated peaks.

(d) Migration Reversal in the BGS Zone. The migration velocity of the stacked analyte zones may be in the direction of the cathode or the anode depending on *x*. Additionally, mixing of zones at B_1[11] lowers the γ, and thus the BGS zone gets a more generous share of the electric field than is expected through calculation using eq 6. The cumulative effect of the shortening of *x* and the mixing of zones during sample matrix backout will therefore cause an increase in $\nu_a(BGS)$. This is illustrated in Figure 2, while the sample matrix was in transit, the direction of the $\nu_a(BGS)$ reverses from positive (toward the cathode) to negative (toward the anode). That is, before a steady current was reached, phenanthene was detected for the second time. Phenanthrene was monitored using the recorded UV spectral absorbance curve, which is shown in Figure 2 as an inset, to assure that the analyte that was detected at first is the same analyte detected again. Furthermore, this result indicates that the electroosmotic flow of the entire liquid could be faster than the $\nu_{ep}(mc,BGS)$ and $\nu_{ep}^*(a,BGS)$ only during the early stages of the backout step. The current plot (Figure 2) is steep at first, indicating a fast electroosmotic flow, then tapers off after roughly 1 min, implying a probable decrease in the electroosmotic flow.

The electroosmotic flow of the entire backout step was measured at different S plug lengths. The BGS was depicted by a 100 mM phosphate buffer (pH 2.5; 7.7 mS/cm) and S was a

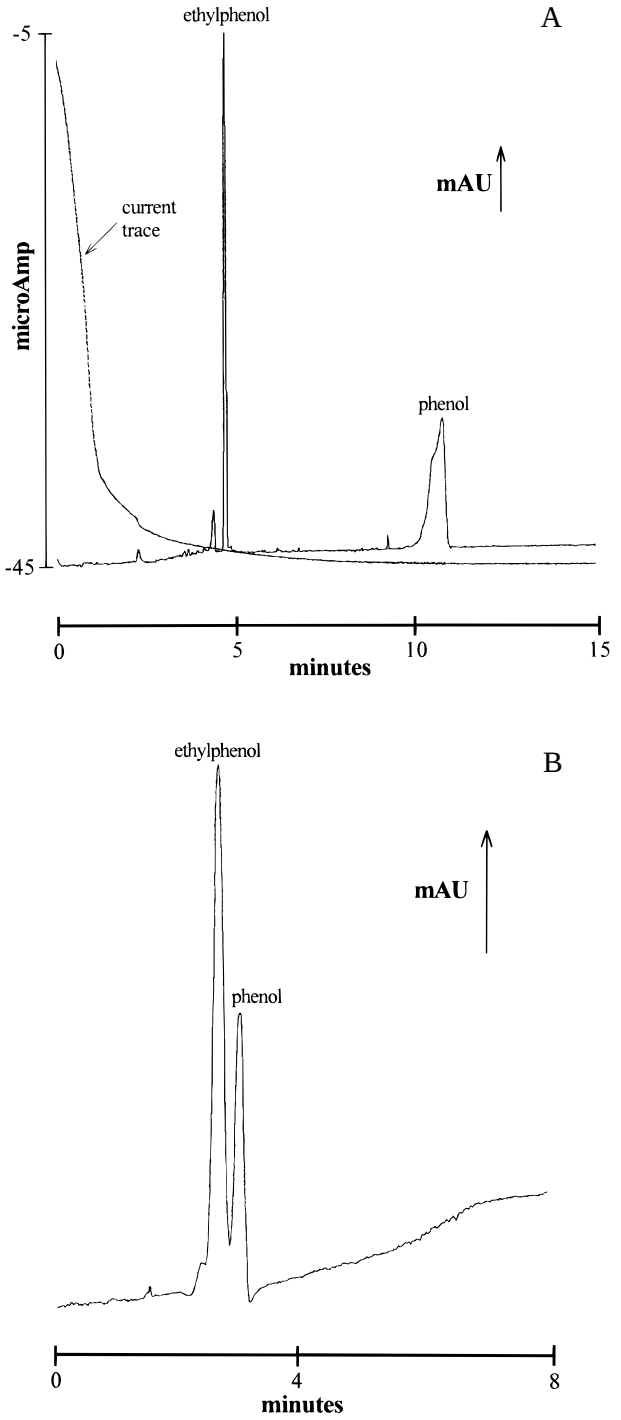

Figure 3. Evidence of the separation of stacked analytes prior to the total removal of the sample matrix: S, ethylphenol and phenol in water; injection, 60 s; stacking and separation regimen, −15 kV throughout the run (A), −15 kV for 90 s followed by pressure at 50 mbar until all peaks are detected (B); data collection, from the application of voltage (A), from the application of pressure (B); other conditions are the same as in Figure 2

1/50-fold dilution of the BGS (0.3 mS/cm). Voltage was applied at −20 kV, and the capillary was 63.5 cm in total length. The time the current stabilized or the time the current reached the predetermined value was taken as the time at which the capillary was voided of the sample matrix. The predetermined value of current was measured with a capillary filled with only BGS. Bear in mind that the measured current of the entire liquid inside the

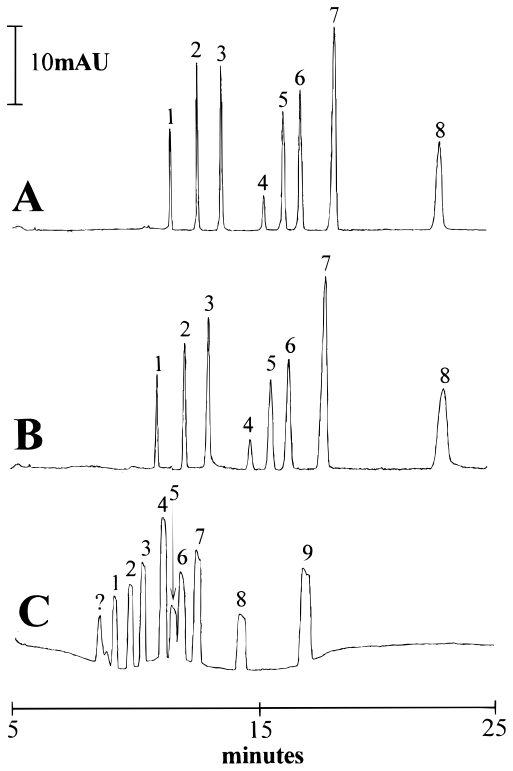

Figure 4. Comparison of peak heights and shapes among different sample matrixes: sample matrix, water (A), 10 mM sodium dihydrogen phosphate (B), 10 mM SDS in water (C); S, phenols (2−10 ppm) in the above sample matrixes; BGS, 100 mM SDS and 1 M urea in 50 mM phosphate buffer (pH 2.5); injection, 30 s; capillary, 66.0 cm (57.5 cm. to the detector); voltage, −20 kV; detection, 210 nm; identification of peaks, consult Table 1

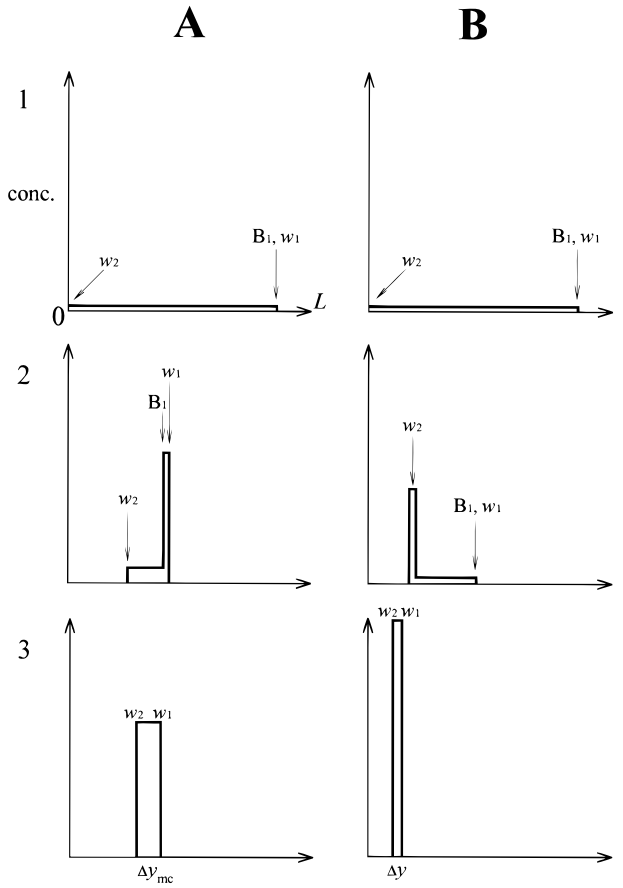

Figure 5. Evolution of the concentration profile of a neutral analyte during stacking: sample matrix, micellar low-conductivity solution (A), nonmicellar low-conductivity solution (B); 1, starting situation; 2, stacking and premature separation of molecules near the concentration boundary (A), analyte molecules being carried to the concentration boundary (B); 3, resultant peak concentration profile after stacking and after the sample matrix was completely removed from the capillary; L, length of the capillary; w_1 and w_2, see text. Note that the positions and shapes of the concentration profiles does not reflect the exact positions and shapes in reality and are only considered as part of many possibilities.

capillary depends on the fractions of S and BGS. The velocity values are approximately 1.3×10^{-2}, 1.1×10^{-2}, 7.2×10^{-3}, 5.9×10^{-3}, and 5.4×10^{-3} cm/s for S plug lengths of 23.3, 7.8, 3.9, 1.9, and 1 cm, respectively. These values support the aforementioned statement regarding the faster electroosmotic flow during the early stages of sample backout.

Choosing the Sample Matrix. As depicted in Figure 4, the presence of micelles in the sample matrix is not necessary for stacking. This was also the case with our earlier studies with NSM and REPSM.[11,12] Conductivities of sample matrixes at 20 °C were 6.0 μS/cm, 1.5 mS/cm, and 0.9 mS/cm for the electropherograms from A to C, respectively. The BGS had a conductivity of 7.9 mS/cm. Stacking effects were similar with A and B although the expected γ was higher with A. Despite the fact that the γ in B would be almost the same as in C, flat topped and broad peaks were observed with C (samples prepared in a sample matrix containing SDS at a concentration greater than its cmc). These results suggest that effective stacking is dependent on not solely the field enhancement in the S zone but also the composition of the sample matrix.

(a) Broadening due to the Presence of Micelles in the S Zone, an Equation To Describe Peak Widths after Stacking. To explain the flat and broad peaks when S contains micelles, let us look at the time for which molecules of a specific analyte reach B_1. Those that are situated near B_1 will reach this boundary earlier than those found near the cathodic vial. Molecules that will stack eventually will leave B_1 before other molecules reach this boundary (see Figure 5A). In the case where S is free of micelles, the time to reach B_1 for most molecules may almost be the same (see Figure 5B).

Consider molecules of a in the S region found at a distance (w) from B_1, the time (t) to reach B_1 for these molecules is given by

$$t = \frac{w}{\nu_a(\mathrm{S}) + \nu_{\mathrm{B1}}} \tag{12}$$

where w is between 0 and xL. Substituting ν_a(S) in eq 8 and ν_{B1} as ν_{eof}(av) to eq 12 then yields

$$t = \frac{w}{\nu_{ep}{}^*(\mathrm{a,S}) + 2\nu_{eof}(\mathrm{av})} \tag{13}$$

As shown in Figure 5A.1 and B.1, let w_1 and w_2 represent the nearest and farthest distance from B_1. In Figure 5A.2, molecules initially found at w_1 have traveled a distance equal to the product

of ν_{ep}*(a,BGS) and the time for transition from (A.1) to (A.2). On the other hand, corresponding molecules in Figure 5B.2 have not yet reached B_1. Let t_1 and t_2 represent the corresponding times when S is free of micelles and t_{1mc} and t_{2mc} represent the corresponding times when S contains micelles. The difference of these times (Δt and Δt_{mc}, eqs 14 and 15, respectively) therefore

$$\Delta t = t_2 - t_1 \tag{14}$$

$$\Delta t_{mc} = t_{2mc} - t_{1mc} \tag{15}$$

represent the time spent in the BGS region by molecules initially found at w_1. This is after the same molecules initially found at w_2 reach B_1. Substituting eq 13 properly into eqs 14 and 15 yields

$$\Delta t = \frac{w_2}{\nu_{ep}*(a,S) + 2\nu_{eof}(av)} - \frac{w_2}{\nu_{ep}(mc,S) + 2\nu_{eof}(av)} \tag{16}$$

$$\Delta t_{mc} = \frac{w_2}{\nu_{ep}*(a,S) + 2\nu_{eof}(av)} - 0 \tag{17}$$

where t_1 is approximated by the time the micelles reach B_1, as given in the second term in eq 16. Assuming complete micellar solubilization, t_{1mc} is 0 since w_1 is approximately 0 because molecules in this case will reach B_1 right after the application of voltage.

From examination of eqs 16 and 17 and assuming that ν_{ep}*(a,S) in both equations are not so different, Δt is therefore less than Δt_{mc} by a factor approximately equal to t_1. The product of ν_{ep}*(a,BGS) and Δt or Δt_{mc} can approximate the length of each analyte band after stacking (Δy and Δy_{mc} given as eqs 18 and 19,

$$\Delta y = \nu_{ep}*(a,BGS)\Delta t \tag{18}$$

$$\Delta y_{mc} = \nu_{ep}*(a,BGS)\Delta t_{mc} \tag{19}$$

respectively), where the contribution of pertinent dispersive effects (e.g., laminar flow produced by the mismatch of local electroosmotic velocities) is neglected. Δy is less than Δy_{mc} since $\Delta t < \Delta t_{mc}$ (Figure 5A.3 and B.3). This explains quantitatively the flat and broader peaks when S contains micelles.

(b) Effect of the Presence of Micelles in S on Migration Times. Migration times are also shorter when S contains micelles (Figure 4C) compared to when S is free of micelles (Figure 4A and B). This is observed to a greater extent with lower retention factor compounds. For instance, phenol (peak 9) which is not detected after 25 min in Figure 4A and B is detected in Figure 4C in less than 18 min. Only the presence of micelles in the S zone makes Figure 4C different from Figure 4B and the direct effect will be on the analyte retention factors. Though this may not be the only reason since the direction of ν_{mc}(BGS) reverses, as stated earlier (among other things). This reversal is still unpredictable and would call for intricate experiments. In any case, the matrix of choice is a nonmicellar solution.

Effect of pH on Stacking. The electroosmotic flow velocity declines with the decrease in pH below 5.5 for SDS micellar systems.[13] With this in mind, the amount of sample that can be stacked will be greater at lower pH given a fixed fraction of the capillary filled with S. As anticipated, relative peak heights of the two naphthalene derivatives increased with the decrease in pH of the run buffer (see Figure 6). The conductivity of the BGSs at the studied pH range did not significantly change. Therefore, the contribution of ionic strength to the electroosmotic flow velocity and γ was negligible. The injection time of 300 s was chosen

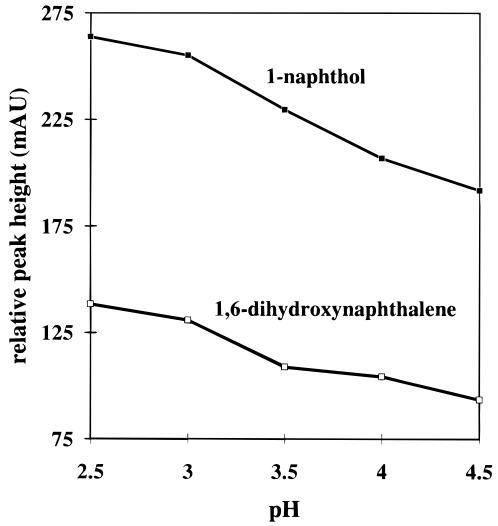

Figure 6. Effect of pH on relative peak heights of selected naphthalene derivatives with stacking: BGS, 100 mM SDS in 50 mM phosphate buffer; sample matrix, water; injection, 300 s; capillary, 63.5 cm (55 cm to the detector); applied voltage, −20 kV; detection, 210 nm.

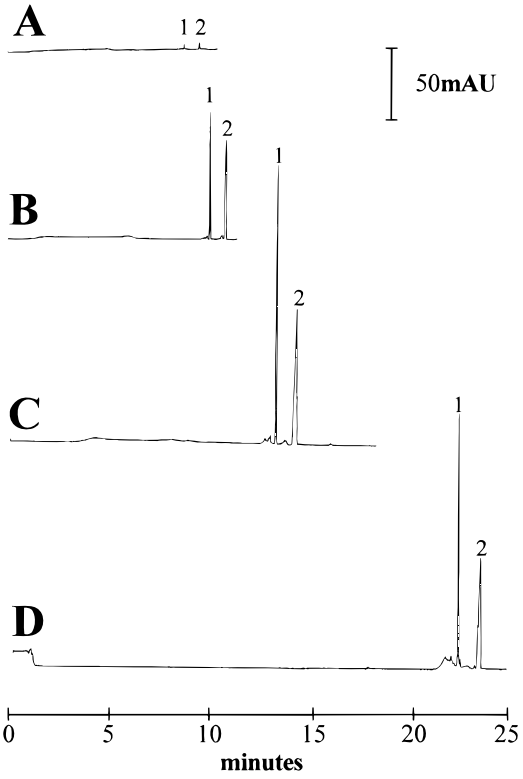

Figure 7. Effect of injection time or sample plug length on peak height enhancements and migration times: injection, 2 (A), 150 (B), and 300 s (C), capillary was filled with sample solution by flushing at 1 bar (D); pH of BGS, 2.5; peak identity, (1) 1-naphthol, (2) 1,6-dihydroxynaphthalene; other conditions are as in Figure 6.

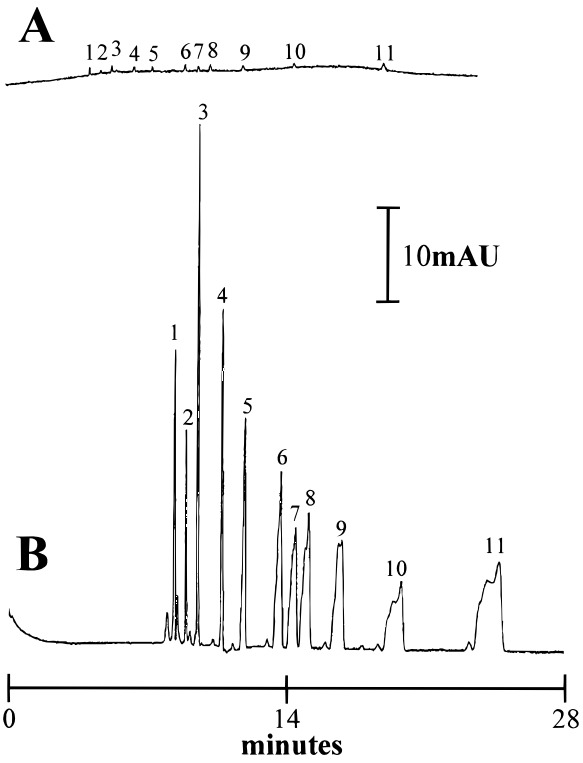

Figure 8. Optimized electropherogram of 11 phenols. injection, 2 s (A), 200 s (B); BGS, 100 mM SDS and 1 M urea in 50 mM phosphate buffer (pH 2.5); S, phenols (1−5 ppm) in water; capillary, 63.5 cm (56 cm to the detector); applied voltage, −22 kV; detection, 210 nm; identification of peaks, see Table 2.

since longer injections at pH 2.5 did not produce further improvement in relative peak heights.

Effect of Sample Plug Length on Peak Height Enhancements and Migration Times. As the amount of sample loaded is increased and stacked, peak heights will logically increase (see Figure 7). However, after a 300 s injection as mentioned earlier, peak heights of the test naphthalene derivatives ceased to increase. This can be explained by the x_{max}* (eq 20), the fraction

$$x_{max}^* = x_{max}\frac{k_S}{k_S + 1} \tag{20}$$

of the capillary filled with S that can only allow the movement and stacking of neutral analytes to the concentration boundary.[12] The higher the x_{max}* the greater the amount of analyte that can be stacked.

Migration times increased with the increase in plug length (see again Figure 7). This phenomenon is mainly due to the backout step. Although ν_{ep}(mc,S) is high, ν_{ep}(mc,BGS) during the backout step is low and probably had a greater contribution to the overall migration time. The overall migration time may be subdivided into three ordered stages: (1) the time the analyte reached B_1; (2) the time the sample matrix was completely removed from the capillary if the analyte was not yet detected; (3) the time the analyte reached the detector. Each stage possesses complex processes. For low retention factor compounds (e.g., phenol), stages 1−3 should all be considered. Notice in Figure 3A that the current has stabilized long enough before phenol was detected.

Table 1. Effect of Retention Factors and Injection Time on Peak Widths[a]

		peak widths (mm)		
peak no.	sample name	2 s	20 s	200 s
1	2,3,5-trimethylphenol	2.7	2.8	2.3
2	*p*-ethylphenol	4.4	3.8	2.4
3	*m*-chlorophenol	2.8	3.0	5.2
4	*o*-chlorophenol	2.6	3.5	3.9
5	4-methylphenol	2.4	3.8	4.3
6	2-methylphenol	2.4	4.3	5.1
7	*p*-nitrophenol	2.7	5.3	6.9
8	*o*-fluorophenol	2.6	5.8	7.3
9	phenol	3.1	6.5	9.5

[a] Conditions: BGS, 50 mM SDS in 50 mM phosphate buffer (pH2.5); S, phenols (5−10 ppm) in water; capillary, 63.5 cm (56 cm to the detector); applied voltage, −27 kV; detection, 210 nm.

High retention factor compounds (e.g., ethylphenol in Figure 3A) may already be detected before the sample matrix is completely removed. A thorough mathematical treatment is needed to foretell migration times of analytes with respect to the volume or length of injected sample. But of course, it is practical to look more at the applicability and transparency of the method rather than simulating or predicting electropherograms.

Effect of Sample Plug Length and Retention Factor on Peak Heights and Peak Widths. Generally, as shown in Figure 8B, peaks are sharp for high retention factor phenols (those that migrate faster) whereas peaks are broad for low retention factor phenols (those that migrate slower) especially phenol and fluorophenol. Peak widths also broadened with the increase in injection time (Table 1). The following discussion will attempt to explain observations regarding the broadening of peaks.

(a) An Equation To Describe Peak Widths Related to *k* for Short-Length Injections of S. Guided by the law of conservation of mass, the concentration of each analyte in the S zone (C_S) is related to the concentration of the stacked analyte in the BGS zone (C_{BGS}) by

$$C_S\nu_{ep}^*(a,S) = C_{BGS}\nu_{ep}^*(a,BGS) \tag{21}$$

Equation 21 is only valid when all injected molecules of the analyte cross B_1. C_S and C_{BGS} can be approximated by eqs 22 and 23,

$$C_S = n/x_{inj}LA \tag{22}$$

respectively, where n is the number of moles of a, x_{inj} is the fraction

$$C_{BGS} = n/\Delta yA \tag{23}$$

of the capillary injected with S, and A is the cross-sectional area of the capillary. Substituting eqs 10, 11, 22, and 23 into equation 21 yields,

$$\frac{n}{x_{inj}LA}\mu_{ep}(mc)\frac{k_S}{k_S+1}\frac{\gamma E_0}{\gamma x + (1-x)} = \frac{n}{\Delta yA}\mu_{ep}(mc) \times \frac{k_{BGS}}{k_{BGS}+1}\frac{E_0}{\gamma x + (1-x)} \tag{24}$$

Table 2. Stacking Enhancement Factors Obtained for the Selected Phenol Derivatives[a]

peak no.	sample name	SE_{height}[b]	SE_{area}[c]
1	amylphenol	43	36
2	*p*-*tert*-butylphenol	91	63
3	2,3,5-trimethylphenol	131	107
4	*p*-ethylphenol	105	70
5	*m*-chlorophenol	74	123
6	*o*-chlorophenol	38	131
7	4-methylphenol	37	107
8	2-methylphenol	39	91
9	*p*-nitrophenol	28	92
10	fluorophenol	20	84
11	phenol	18	99

[a] Conditions are the same as those in Figure 9. [b] $SE_{height} = H_{stack}/H$ = (height obtained with stacking)/(height obtained from a 2 s injection). [c] $SE_{area} = A_{corr,stack}/A_{corr}$ = (corrected area obtained with stacking)/(corrected area obtained from a 2 s injection).

Table 3. Calibration Curves, Concentration Detection Limits, and RSD (%) for the Studied Naphthalene Derivatives[a]

	injection	
	2 s	250 s
	1. Equation of the Line	
a. 1-naphthol	$y = 2.0941x + 1.0568$ $r = 0.9984$	$y = 3.3157x + 0.9991$ $r = 0.9986$
b. 1,6-dihydroxy-naphthalene	$y = 1.9929x + 1.0272$ $r = 0.9976$	$y = 2.9267x + 0.9817$ $r = 0.9969$
	2. Limit of Detection Computed on the Basis of Peak Height (S/N 3)	
a. 1-naphthol	1.38×10^{-6} M	3.67×10^{-8} M
b. 1,6-dihydroxy-naphthalene	1.14×10^{-6} M	6.75×10^{-8} M
	3. RSD (%) ($n = 9$)	
i. migration time		
a. 1-naphthol	0.42	6.74
b. 1,6-dihydroxy-naphthalene	0.30	6.25
ii. peak height		
a. 1-naphthol	18.77	7.01
b. 1,6-dihydroxy-naphthalene	18.26	5.04
iii. peak height ratio	2.46	5.28

[a] *y*, logarithm (height); *x*, logarithm (M); concentration range, 6.46×10^{-4}–4.36×10^{-6} M; peak height ratio, peak height of 1-naphthol/peak height of 1,6-dihydroxynaphthalene; conditions are the same as those found in Figure 7C.

Table 4. Calibration Curves, Concentration Detection Limits, and RSD (%) for the Studied Steroids[a]

	hydrocortisone	cortisone	testosterone
1. *y* intercept	0.7010	0.7340	0.7104
2. slope	−0.2135	−0.0513	−0.0939
3. *r* value	0.9782	0.9774	0.9773
4. limit of detection (S/N 3)			
a. ppb	19.35	14.15	13.84
b. $\times 10^{-8}$ M	5.34	3.93	7.29
5. % RSD			
a. migration time ($n = 15$)	2.83	2.76	2.54
b. peak height ratio ($n = 4$)	3.33	1.87	3.38

[a] Equation of the line, log(peak height ratio) = slope[log (ppm concentration)] + *y*-intercept; peak height ratio, peak height of the sample/peak height of internal standard; concentration range, 12.5–0.1055 ppm; conditions same as those found in Figure 9.

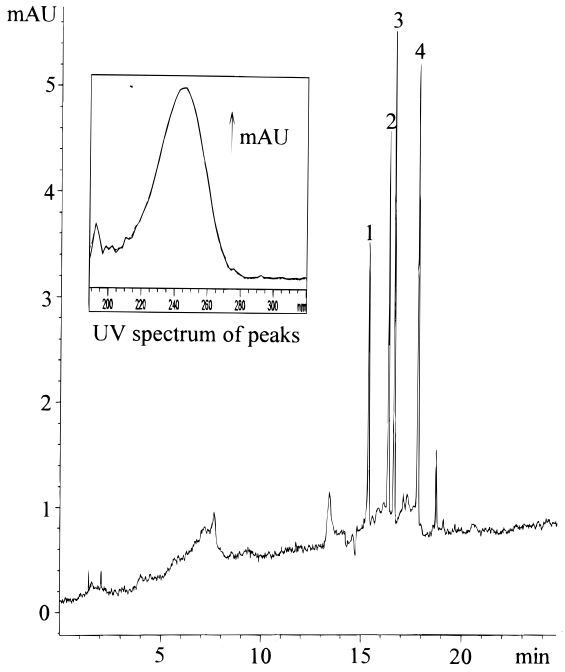

Figure 9. Electropherogram of the four steroids studied: BGS, 100 mM SDS and 40 mM γ-cyclodextrin in 50 mM phosphate buffer (pH 2.5); S, sample stock solutions diluted with water; voltage, −20 kV; detection, 247 nm; injection, 350 s; peak identification, (1) progesterone, (2) hydrocortisone, (3) cortisone, (4) testosterone; concentration of samples, ~1 ppm; capillary, 63.5 cm (55 cm to the detector). The inset is an on-line recorded spectrum that is characteristic at each peak maximum.

After rearrangement, a new relation for Δy is then derived as

$$\Delta y = \frac{x_{inj} L}{\gamma} \frac{k_S + 1}{k_S} \frac{k_{BGS}}{k_{BGS} + 1} \qquad (25)$$

This relation also neglects the contribution of pertinent dispersive effects and is only true for short injections of S ($x_{inj} < x_{max}$*). Since k_{BGS} is directly related to k_S and $k_{BGS} \gg k_S$, Δy will therefore be longer for low-*k* compounds compared to high-*k* compounds. This explains the wider peak widths with low-*k* compounds (Table 1, 20 s injection).

(b) Explanations of the Effect of Longer Injections of S on Peak Widths. The values of x_{max}* are shorter for low retention factor compounds than those with high retention factors based on eq 20. If a capillary is filled with S to a fraction greater than each analyte's x_{max}*, micelles will only enter the S zone without carrying any neutral analyte until x_{max}* of any compound is reached. Some samples are then lost to the inlet vial. Before neutral analytes migrate toward the anode, micelles will therefore be present in the S region. This now becomes the same argument about the results on Figure 4 with samples prepared in a matrix with micelles. Together with the discussion in the previous paragraph, these explain the wider peak widths for low-*k* compounds and longer injections of S (Table 1, 200 s injection).

Stacking Enhancement Factors Obtainable with the Stacking Procedure. Stacking enhancement factors in terms of height and area,[12] SE_{height} and SE_{area}, respectively, are simply the peak heights and corrected peak areas obtained with stacking divided

by the corresponding values obtained with the usual injection procedure. Calculated values for 11 phenol derivatives using the optimized electropherogram (Figure 8B) are given in Table 2. Values of more than 100 for SE_{height} and SE_{area} are observed with some phenols. Remember that a value of 100 for SE_{height} corresponds to 2 orders of magnitude improvement in concentration detection limit. Currently, we are trying to improve the peak shapes of low-*k* analytes by working on higher concentrations of SDS without compromise to the resolution of high-*k* analytes and by investigating polymer surfactants with zero cmc that have properties like SDS in acidic buffers.

Application to Qualitative and Quantitative Analysis. From the comparison between the 2 and 250 s (sample stacking) injections, almost 2 orders of magnitude improvement in concentration detection limit was achieved with the test naphthalene derivatives (see Table 3). A problem encountered with the stacking and normal injection procedure is the irreproducibility of peak heights, which is solved by employing peak height ratios or utilizing the internal standard technique as done with the steroids in this study. A probable reason is the fluctuation of the electroosmotic flow. With progesterone as internal standard, concentration detection limits of hydrocortisone, cortisone, and testosterone are all less than 20 ppb (see Table 4). A sample electropherogram of the studied steroids with very sharp peaks is shown in Figure 9. The spectral absorbance curve is also included which guided us in the analysis. Although the computed statistical values given in Tables 3 and 4 are not so spectacular for this stacking procedure, we believe that this technique can be broadly used for actual analysis.

CONCLUSION

This stacking procedure in reversed migration-MEKC with hydrodynamic injection is easy, fast, and effective. Detection sensitivity can be enhanced more than a 100-fold and concentration sensitivity improved more than 1 order of magnitude. Moreover, detection limits are now comparable to those obtained from high-performance liquid chromatography. Small amounts of organic solvent in the sample matrix did not produce undesirable effects to the stacking method. Compared with NSM and REPSM, aside from greater enhancements in detection, plate heights are still astounding (reaching 1 million plates with high *k* analytes). Moreover, stacking and separation conditions for complex samples like the 11 phenols presented are easy to establish. Regarding analysis of real samples (e.g., analytes in biological or forensic matrixes), neutral and anionic constituents present in such sample matrixes can mask the stacking effects of this procedure; thus, a sample cleanup step prior to stacking is deemed necessary. A design utilizing solid-phase extraction or liquid−liquid extraction preceding this stacking procedure is currently being explored for the analysis of some real samples. At the end, we believe that this is a major step in making MEKC a more universal analytical tool.

ACKNOWLEDGMENT

The authors are thankful to Dr. P. Muijselaar for checking the manuscript and Drs. K. Otsuka and N. Matsubara for the support. J.P.Q. is also grateful to the Ministry of Education, Science, Culture, and Sports, Japan for the scholarship and the University of the Philippines Manila for allowing him to go on leave. This work was supported in part by a Grant-in-Aid for Scientific Research (No. 07554040) from the Ministry of Education, Science, Culture, and Sports, Japan.

Received for review June 18, 1997. Accepted October 14, 1997.[⊗]

AC9706281

[⊗] Abstract published in *Advance ACS Abstracts,* December 1, 1997.